Journal of Biomedical Optics

SPIEDigitalLibrary.org/jbo

Advanced chemical imaging and comparison of human and porcine hair follicles for drug delivery by confocal Raman microscopy

Lutz Franzen
Christiane Mathes
Steffi Hansen
Maike Windbergs

SPIE

Advanced chemical imaging and comparison of human and porcine hair follicles for drug delivery by confocal Raman microscopy

Lutz Franzen,[a*] Christiane Mathes,[a*] Steffi Hansen,[a,b] and Maike Windbergs[a,b,c]
[a]Saarland University, Department of Biopharmaceutics and Pharmaceutical Technology, Saarbruecken, Germany
[b]Helmholtz Institute for Pharmaceutical Research Saarland, Helmholtz Center for Infection Research, Saarbruecken, Germany
[c]PharmBioTec GmbH, Saarbruecken, Germany

Abstract. Hair follicles have recently gained a lot of interest for dermal drug delivery. They provide facilitated penetration into the skin and a high potential to serve as a drug depot. In this area of research, excised pig ear is a widely accepted *in vitro* model to evaluate penetration of drug delivery into hair follicles. However, a comparison of human and porcine follicles in terms of chemical composition has not been performed so far. In this study, we applied confocal Raman microscopy as a chemically selective imaging technique to compare human and porcine follicle composition and to visualize component distribution within follicle cross-sections. Based on the evaluation of human and porcine Raman spectra optical similarity for both species was successfully confirmed. Furthermore, cyanoacrylate skin surface biopsies, which are generally used to determine the extent of follicular penetration, were imaged by a novel complementary analytical approach combining confocal Raman microscopy and optical profilometry. This all-encompassing analysis allows investigation of intactness and component distribution of the excised hair bulb in three dimensions. Confocal Raman microscopy shows a high potential as a non-invasive and chemically selective technique for the analysis of trans-follicular drug delivery. [DOI: 10.1117/1.JBO.18.6.061210]

Keywords: hair follicle; dermal drug delivery; confocal Raman microscopy; optical profilometry; human skin; porcine skin.

Paper 12603SS received Sep. 11, 2012; revised manuscript received Oct. 22, 2012; accepted for publication Oct. 23, 2012; published online Nov. 19, 2012.

1 Introduction

The trans-follicular route for drug administration has gained a lot of attention in recent years, mainly driven by the advent of nanoparticle-based delivery systems facilitating absorption into hair follicles. Current research efforts span a broad field of different applications ranging from cosmetic products for acne treatment up to transcutaneous vaccination.[1–3] Different aspects contribute to the attractiveness of the hair follicle for drug delivery. Anatomically, the hair follicle embodies an invagination of the epidermis resulting in an increased surface area available for penetration and absorption of drugs surrounded by numerous blood capillaries facilitating systemic absorption. Furthermore, the presence of antigen presenting cells as, for instance, Langerhans cells bears the potential to provoke an immune response.[3,4] In addition, the hair follicle was found to provide a long-term drug reservoir for up to 10 days.[5]

The development of novel drug delivery systems for trans-follicular delivery necessitates a suitable model for *in vitro* absorption and penetration studies into the hair follicle. For skin absorption and percutaneous penetration testing, porcine skin has been evaluated as a valuable *in vitro* model.[6] Yet, for trans-follicular drug delivery it is important to know whether explicitly porcine hair follicles are suitable for simulating the human hair follicle. As far as the anatomical comparison, both follicles show an inner and outer root sheath, a sebaceous gland associated with the hair follicle and sweat glands in the dermal layer.[7,8] The thickness of the stratum corneum and the viable epidermis as well as density and follicle diameter of the hairs were found to be similar.[7] By using the skin sandwich method, it was demonstrated that porcine hair follicle absorption of different solutes varying in their physicochemical properties matches previously accumulated absorption data into the human hair follicle.[9] Furthermore, in contrast to human skin, porcine ear cartilage prevents contraction of tensile fibers and subsequent closure of the hair follicles, thus corroborating the applicability of a porcine model.

To analyze the extent of follicular drug penetration, the state of the art procedure is cyanoacrylate skin surface stripping. This technique implies the application of superglue to a predetermined skin area covered by a tape strip. Upon polymerization of the glue, the tape strip is quickly peeled off, removing corneocytes, the stratum corneum and the follicular cast.[10] These biopsies are subsequently extracted and the content of penetrated drugs is analytically quantified.

Several studies have already shown evidence that percutaneous absorption in pig skin is equivalent to that in human skin.[7,11] However, because the sebum within the hair follicle forms the release medium for drugs delivered via the trans-follicular route, the equivalency of human and porcine sebum is quite important. The different components that constitute

*These authors contributed equally to this work.

Address all correspondence to: Maike Windbergs, Saarland University, Department of Biopharmaceutics and Pharmaceutical Technology, Campus A4 1, Saarbruecken, Germany; Helmholtz-Institute for Pharmaceutical Research Saarland (HIPS), Department of Drug Delivery, Saarbruecken, Germany. Tel: +49 681 302 2358; Fax: +49 681 302 4677; E-mail: m.windbergs@mx.uni-saarland.de

0091-3286/2013/$25.00

sebum in humans, rats, mice and hamsters have been assessed showing that it is gerenally composed of triglycerides, sterol- or wax-esters, diol-diesters, free sterols, and free fatty acids. However, only human sebum contains squalene.[9,12] Unfortunately, according to our knowledge there is no literature about the composition of porcine sebum.

Even though the porcine hair follicle is widely used as an *in vitro* model simulating the human follicle, an all-encompassing comparison in terms of chemical composition has not been performed so far. A suitable technique for a chemically selective and nondestructive analysis of such samples is confocal Raman microscopy. Besides a spectroscopic analysis of the individual chemical composition, confocal Raman microscopy offers the possibility of sample mapping, thus facilitating the visualization of spatially resolved component distribution. So far, confocal Raman microscopy was used for qualitative follow-up of substances into skin *in vivo*[13] as well as *in vitro*.[14,15] Furthermore, Raman microscopy has proven its suitability to map substance distribution on the skin surface.[16] Recently, studies visualized human hair composition, gaining information about protein secondary structure and disulfide cross-links.[17]

In this study, we apply confocal Raman spectroscopy to evaluate the chemical similarity of human and porcine hair follicles. For this purpose, we compare the spectral properties of the four main follicle-associated components—hair, sebum, dermis and follicular epidermis. Furthermore, confocal Raman microscopy is used to image follicle cross sections, visualizing the component distribution. Finally, the novel complementary analytical approach of confocal Raman and optical profilometry is used to visualize cyanoacrylate biopsies of hair follicles in three dimensions.

2 Materials and Methods

2.1 *Materials*

Tesafilm® kristall-klar (Tesa, 33 m × 19 mm, cut to pieces of 30 × 19 mm) was purchased from Tesa AG, Hamburg, Germany. UHU superglue (UHU, blitzschnell Pipette) was provided by UHU GmbH & Co, KG, Bühl/Baden, Germany. Mayer's haematoxylin was obtained from Carl Roth GmbH+ Co. KG, Karlsruhe, Germany.

2.2 *Porcine Skin*

Fresh pig ears were obtained from Emil Färber GmbH & Co. KG, Zweibrücken, Germany. The ears were excised before brewing and shipped immediately to the lab. After rinsing with water, they were inspected for evident skin abrasions prior to use. Only healthy-looking skin was selected for the experiments.

2.3 *Human Skin*

Fresh human skin for the *in vitro* experiment was obtained from plastic surgery of female Caucasian patients from the department of Plastic and Hand Surgery, Caritaskrankenhaus, Lebach, Germany. The study included thigh skin from a female donor, 48 years old, previously consented. Immediately upon arrival of the skin, the subcutaneous adipose tissue was removed with a scalpel and the skin was cut into pieces of 10 × 20 cm, wrapped in aluminum foil and stored in polyethylene bags at −20°C until use. The study was approved by the ethical commission of Saarland, Germany (Aerztekammer des Saarlandes, 204/08).

2.4 *Cross-Sections of Hair Follicle*

To get a cross section of a hair follicle, a biopsy of a 20 × 30-mm sample was cut out of the intact frozen thigh skin using a scalpel and cross-sections with a thickness of 15 μm were cut using a cryomicrotome (MEV Cryostat, Slee, Mainz, Germany). Nuclear staining was performed using Mayer's haematoxylin. The optical microscope images were taken using a Zeiss AXIO Scope A1 light microscope (Carl Zeiss Microscopy GmbH, Oberkochen, Germany) equipped with a digital camera (AxioCam ERc 5 s). Images were edited and labeled using the software Zen lite 2011 (Carl Zeiss Microscopy GmbH, Oberkochen, Germany).

2.5 *Cyanoacrylate Skin Surface Stripping*

Cyanoacrylate skin surface biopsies were taken by applying a drop of superglue on a predetermined and precleansed location of the excised pig ear, immediately followed by application of a tape strip on top.[10,18] After polymerization of the glue (15 min), this tape was quickly removed along with the content of the hair follicle. For analysis the biopsies were fixed upside down on glass slides, leaving the follicles sticking up.

2.6 *Confocal Raman Microscopy*

For confocal Raman microscopic evaluation, cross-sections and cyanacrylate biopsies were placed on calcium fluoride slides. Measurements were performed using a Witec alpha 300*R*+ (WITec GmbH, Ulm, Germany). The excitation source was a diode laser with an emitting wavelength of 785 nm. Laser power was adjusted to 50 mW before the objective, which was found to be harmless to biological tissue. Microscopic images were obtained with a 10× objective (Epiplan Neofluar N.A. 0.5, Zeiss, Germany). Raman single spectra and maps were recorded with a 50× objective (Epiplan Neofluar N.A. 0.8, Zeiss, Germany). A confocal pinhole of 100 μm rejected signals from out-of-focus regions. Raman spectra were recorded in the range of 400 to 1780 cm^{-1} with a spectral resolution of 4 cm^{-1}. For single spectra, three measurements over a 10-s integration time were averaged. Raman mapping was performed by collecting data for 10 s every 5 μm in x and y directions. The data were processed using WITec Project Plus software (WITec GmbH, Ulm, Germany). After cosmic ray removal, the spectral baseline was corrected using a polynomic fit. All spectra were normalized to the most intense peak (1430 to 1480 cm^{-1} representing ν(C—H).[19]

2.7 *Optical Profilometry*

Surface topography measurements were performed with a True Surface Microscopy sensor integrated in a Witec alpha 300*R*+ confocal Raman microscope (WITec GmbH, Ulm, Germany). The sensor can resolve an elevation difference of 3 mm, with an accuracy of 1 μm. Data points were recorded every 5 μm in x and y directions, generating a lateral resolution equivalent to Raman mapping.

3 Results and Discussion

3.1 *Comparison of Porcine and Human Hair Follicles*

Porcine ear skin represents a commonly used model for analysis of drug penetration into hair follicles. However, besides

anatomical and physiological similarity one major aspect for the applicability of such a model is the chemical equivalence with the simulated site in the human body. Thus, in order to verify the suitability of porcine follicles as an *in vitro* substitute for human follicles, a comparison of the composition of major chemical components is performed by confocal Raman spectroscopy.

Optical and dimensional similarity of porcine and human hair follicles and the adhering tissue are depicted as microscopic sections in Fig. 1(a) and 1(b), respectively. The hair (blue cross), follicular epidermis (yellow cross), deeper skin layers (green cross), and the sebaceous gland (red cross) are clearly visible in the individual cross-sections. To evaluate the spectral comparability, Raman spectra were obtained from the four regions of interest marked by the colored crosses. Raman spectra recorded from porcine and human dermis (green), hair (blue), follicular epidermis (yellow) and a sebaceous gland (red) are depicted in Fig. 1(c) and 1(d), respectively (colored figures available online only). The follicular epidermis spectrum is composed of unspecific bands representing protein at around 1003 cm^{-1} (aromatic amino acids), at 1440 cm^{-1} δ(CH) and at 1650 cm^{-1} (amide I) with keratin as the main component.[19] The dermis spectrum is additionally characterized by two double peaks at 815 to 850 cm^{-1} and 920 to 940 cm^{-1}. This pattern is representative for collagen, which is localized in the dermis in significantly higher quantities than in other tissue regions.[20] Human and porcine hair reveal a prominent peak at 509 cm^{-1} specific for $S-S$ cross-links, which appear in high content in keratotic tissues like horn, hoof, and hair.[17,21] To evaluate the recorded spectra of human and porcine hair follicle components regarding similarity, a statistically meaningful method is necessary. Therefore, spectral subtraction and calculation of the area under the curve (AUC) of the resulting graphs are performed. As references, three spectra for each component from different positions were subtracted from each other. This generates graphs specifying the internal spectral variability for each individual component. Figure 2(a) depicts these graphs for hair in blue, follicular epidermis in yellow, dermis in green, and sebum in red (colored figures available online only). The confidence interval (CI) of spectral similarity for each individual component is subsequently calculated based on the absolute AUC of these graphs deriving mean and standard deviation. Finally, component spectra of human and porcine follicles are subtracted from each other and AUC of the resulting graph was determined. The calculated AUC of these graphs as well as the confidence interval for spectral similarity are listed in Fig. 2(b). The graph representing the hair states a significantly higher AUC than the reference. However, a direct comparison of the subtracted spectra, as shown in Fig. 2(c) reveals no major discrepancies but high noise. Moreover, the internal variability of the reference measurement for hair is rather small, explaining the detected difference. For follicular epidermis and dermis, no significant difference is exposed. Noteworthy is the high variability in epidermal spectra. This can be explained by the different follicular epidermal layers. To assure robustness of our method, epidermal spectra were taken from different layers. Paying special attention to the sebum as the potential release medium for drug carrier systems, no significant difference in Raman spectra is noted between human and porcine sebum. However, the direct spectral comparison displayed in Fig. 2(d) exhibits a slight heartbeat shaped discrepancy between 1050 and 1090 cm^{-1}. Even though not significantly different, this result indicates a peak shift in the initial spectra from mainly *trans* conformational C—C stretch vibrations in porcine to more random conformations in human sebum. The characteristic peak shift from 1060 to 1080 cm^{-1} of the ν(C—C) skeletal vibrations confirms these findings.[22] Other small discrepancies are intensity related and hint at negligible concentration differences of sebum components. Finally, the inter-individual variability of human and porcine skin composition was not taken into account since a vast number of individuals need to be tested to gain valid results. Yet, Raman spectroscopy has proven its value to compare chemical composition of all main hair follicle components

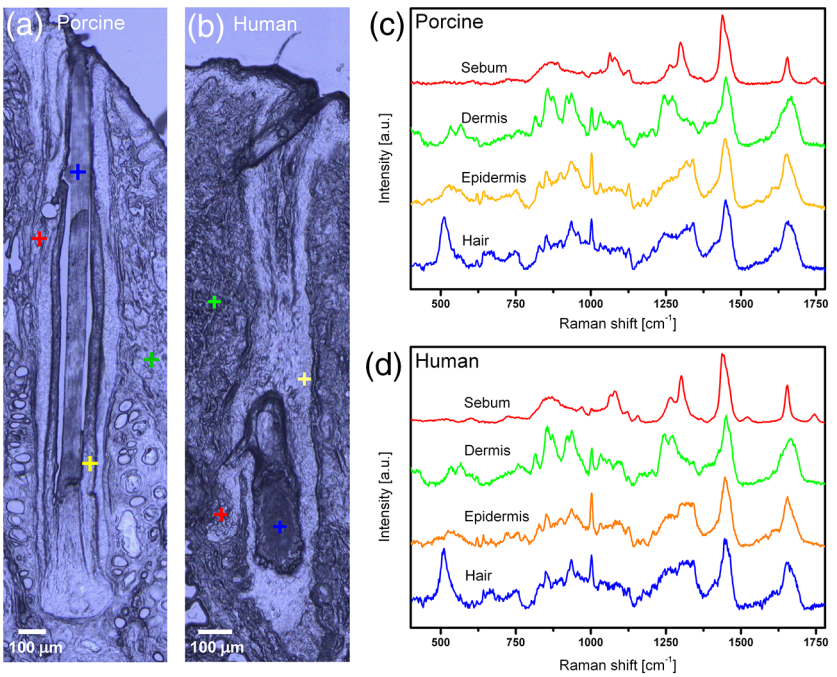

Fig. 1 Microscopic pictures of porcine (a) and human (b) hair follicle cross-sections. Raman spectra obtained from the areas marked by the colored crosses displayed in corresponding colors from porcine (c) and human (d) follicles.

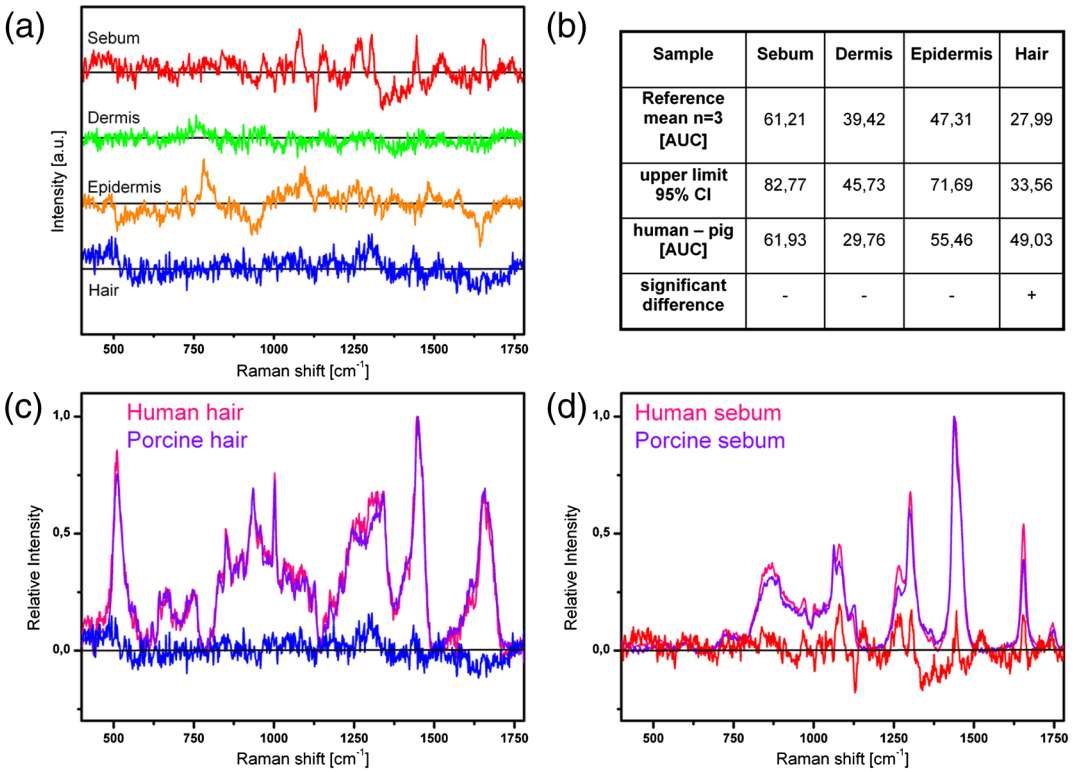

Sample	Sebum	Dermis	Epidermis	Hair
Reference mean n=3 [AUC]	61,21	39,42	47,31	27,99
upper limit 95% CI	82,77	45,73	71,69	33,56
human – pig [AUC]	61,93	29,76	55,46	49,03
significant difference	-	-	-	+

Fig. 2 (a) Spectral subtraction graphs derived from porcine and human Raman spectra of the four main chemical components. (b) Statistical evaluation of the absolute area under the curve (AUC) of the spectral subtraction graphs. Comparison of single Raman spectra and the subtraction graphs for human and porcine hair (c) and sebum (d).

and indicates chemical similarity of the different tissues and sebum in particular.

3.2 *Raman Mapping of Follicle Cross-Sections*

For visualization of different tissue components staining procedures represent the most common technique. Figure 3(a) shows a porcine hair follicle cross-section after haematoxylin nuclear staining. A clear differentiation between follicular epidermis, dermis, and hair is possible. The location of a sebaceous gland can be assumed (red arrow) but the sebum remains undetectable. Raman mapping allows the discrimination of different components according to their Raman spectra without staining, visualizing the component distribution. An unstained microscopic section of a porcine hair follicle is displayed in Fig. 3(b). Raman spectra are recorded from the area indicated by the red rectangle in the image with a step size of 5 μm. After processing the spectral data with multivariant analysis algorithms to identify the component distribution, a false color Raman image is obtained allocating each picture pixel with a color representing similar Raman spectra [Fig. 3(c)]. In this binary method, all spots with spectra representing the dermis are shown in green, follicular epidermis in yellow, hair in blue, and sebum in red. In this image, each pixel is explicitly assigned to a component.

Figure 3(d) depicts the same area after further data processing. This approach displays intensity differences and allows displaying multiple components simultaneously in one pixel. This procedure facilitates a more detailed depiction of the component distribution. A close comparison of Fig. 3(c) and 3(d) reveals the advantages of this more sophisticated method. For instance, traces of sebum (red) can be identified on top of the hair (blue), which is not visible by the binary approach (colored figures available online only). The sebum is mainly located in the sebaceous gland and along the hair shaft. Slight traces of sebum remaining on the hair are considered artifacts generated by the cutting procedure. The Raman map successfully allows insight into the follicle's constitution not feasible by conventional microscopy. Raman microscopy enables visualization and characterization of the follicle's most important components without any labeling or staining. Furthermore, the methodology bares a high potential to track penetration of drugs and drug delivery systems in the follicular tissue.

3.3 *Visualization of Cyanoacrylate Skin Surface Biopsies*

Cyanoacrylate skin surface stripping represents the most common analytical technique to analyze the penetration behavior of drug delivery systems into hair follicles. Removing the hair and the follicular cast as a cyanoacrylate biopsy allows extraction and quantification of penetrated drugs. However, the quality and extent of follicle removal cannot be analyzed with this procedure. Microscopy analysis of a follicle biopsy reveals limitations, as conventional light microscopy only gains information from one focal plane at a time. Figure 4(a) and 4(b) displays two light microscopic pictures obtained from two different focal planes of a porcine cyanoacrylate biopsy visualizing this problem. The biopsy tape is turned upside down with the excised hairs pointing upwards. Only fractions of the hairs can be assessed this way. To evaluate the complete follicle, a three-dimensional analytical approach is necessary.

A versatile method for analysis of structured samples is optical profilometry. The basic principle relies on the effect of chromatic aberration. With a set of hyperchromatic lenses

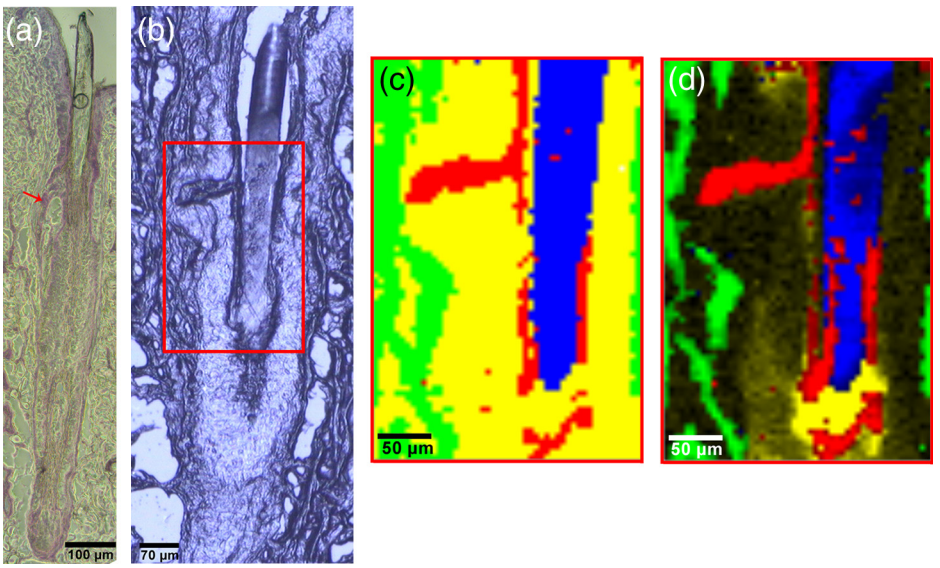

Fig. 3 (a) Transmittance-light microscopy pictures of a haematoxylin nuclear stained porcine hair follicle cross-section. The red arrow indicates the location of the sebaceous gland. (b) Incident light microscopic picture of an unstained porcine follicle cross-section. (c) and (d) Raman map of the area indicated by the red rectangle in (b). The hair is displayed in blue, the sebum is depicted in red, whereas epidermal and dermal structures are shown in yellow and green, respectively.

good mapping-point capabilities are associated with a high chromatic error. Thus, white light which is focused through this lens assembly is split in its different colors, assigning different focal lengths to each color. While detecting the reflected light through a confocal pinhole, a topography map can be generated as displayed in Fig. 4(c). By applying the aforementioned methodology, the complete cyanoacrylate biopsy with the excised hairs can be visualized [Fig. 4(d)].

In a second step, this method allows overlaying the sample surface topography map with Raman spectroscopic information. After determining the surface structure, Raman spectra can be obtained from the exact sample surface eliminating weak signal

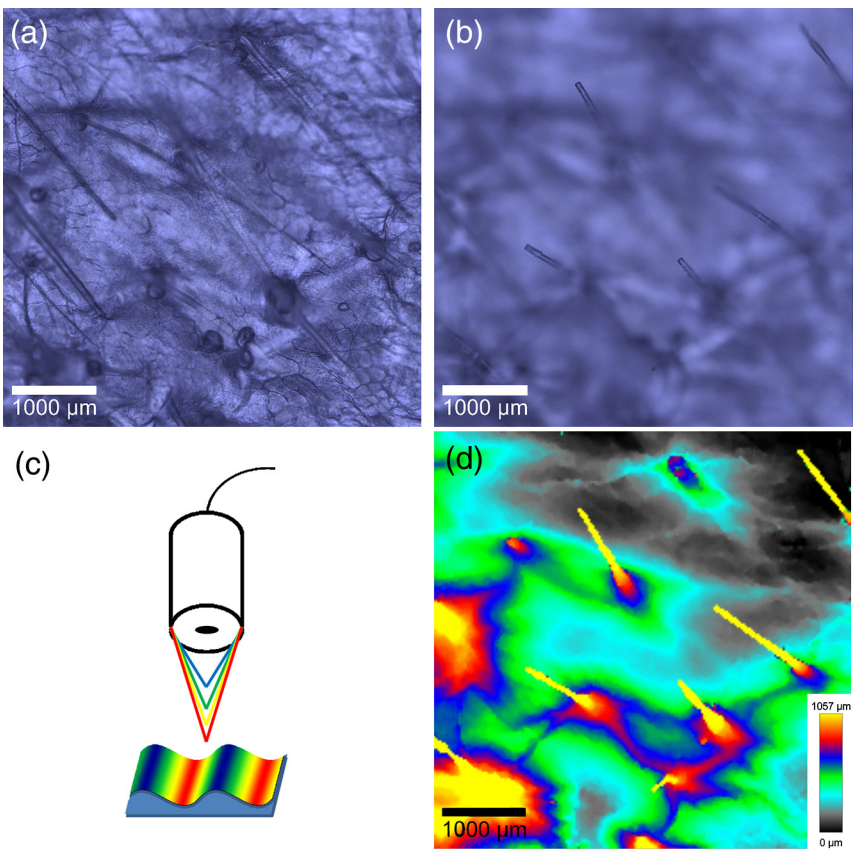

Fig. 4 (a) and (b) depict light microscopy pictures of a cyanoacrylate skin surface biopsy recorded from two different focal planes. (c) Schematic of the basic principle of optical profilometry. (d) Color-coded surface map of the biopsy area corresponding to (a) and (b).

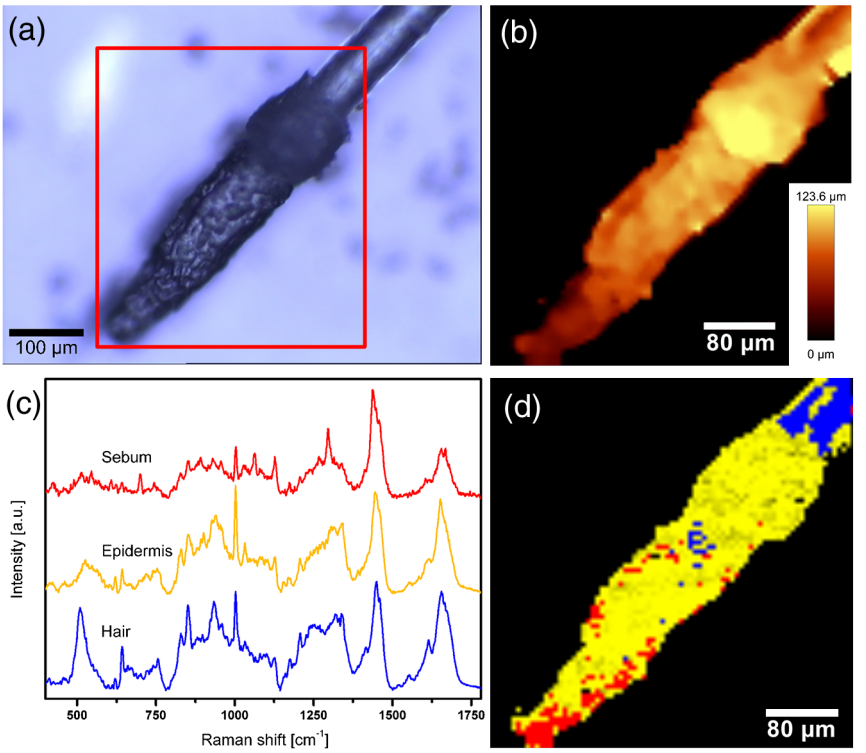

Fig. 5 (a) Light microscopy picture of an excised hair follicle. (b) Surface topography map of the area indicated by the red rectangle in (a). (c) Raman spectra of the individual chemical components in the hair follicle. (d) Raman map displaying the component distribution on the excised hair follicle.

intensity caused by out of focus effects. This enables Raman mapping of highly structured specimen. In this study, the technique was utilized to image a hair follicle obtained from a cyanoacrylate surface biopsy. Figure 5(a) shows a microscopic picture of a single hair bulb. In the area indicated by the red rectangle, the surface structure was assessed by optical profilometry. The resulting topography map of the follicle is presented in Fig. 5(b). The individual Raman spectra of the chemical components within a hair bulb are displayed in Fig. 5(c). Overlaying the surface topography map with the spatially resolved Raman spectral information results in a three-dimensional component distribution map of the follicle [Fig. 5(d)]. The false color image displays hair in blue, sebum in red and epidermal structures in yellow, thus matching the color of the component spectra displayed in Fig. 5(c).

The image depicts an intact follicular epidermis shell enclosing the hair root. Traces of sebum can be found outside the shell, indicating the location of the sebaceous gland. An enhanced sebum presence at the bottom might indicate thinner layers of follicular epidermis at the lower hair bulb. The analytical evidence of the extraction of complete hair bulbs by cyanoacrylate skin surface biopsies corroborates the suitability of this technique for quantification of drugs within the hair follicle.

Furthermore, the novel combination of optical profilometry and confocal Raman microscopy proves its value for the evaluation of skin biopsies and indicates its potential for other analytical approaches.

4 Conclusion

Confocal Raman microscopy proves its enormous potential for nondestructive, chemically selective analysis and evaluation of trans-follicular drug delivery. The comparison and evaluation of human and porcine hair follicles based on their individual Raman spectra successfully indicates their similarity. Besides component distribution analysis within cross-sections, the novel combination of optical profilometry and confocal Raman microscopy allows three-dimensional chemically resolved imaging of cyanoacrylate skin surface biopsies. These results indicate the potential of this analytical approach to visualize penetration behavior of drug delivery systems in follicles as well as for noninvasive depth profiling as a future perspective.

Acknowledgments

We thank L. Muijs for technical support and K.-H. Kostka from Caritas Hospital, Lebach, Germany, for providing human skin.

References

1. L. Mu and R. L. Sprando, "Application of nanotechnology in cosmetics," *Pharm. Res.* **27**(8), 1746–1749 (2010).
2. A. A. Date, B. Naik, and M. S. Nagarsenker, "Novel drug delivery systems: potential in improving topical delivery of antiacne agents," *Skin Pharmacol. Phys.* **19**(1), 2–16 (2006).
3. S. Hansen and C. M. Lehr, "Nanoparticles for transcutaneous vaccination," *Microb. Biotechnol.* **5**(2), 156–167 (2012).
4. V. M. Meidan, M. C. Bonner, and B. B. Michniak, "Transfollicular drug delivery—is it a reality?," *Int. J. Pharm.* **306**(1–2), 1–14 (2005).
5. J. Lademann et al., "Hair follicles—a long-term reservoir for drug delivery," *Skin Pharmacol. Phys.* **19**(4), 232–236 (2006).
6. Y. Frum, G. M. Eccleston, and V. M. Meidan, "*In-vitro* permeation of drugs into porcine hair follicles: is it quantitatively equivalent to permeation into human hair follicles?," *J. Pharm. Pharmacol.* **60**(2), 145–151 (2008).
7. U. Jacobi, "Porcine ear skin: an *in vitro* model for human skin," *Skin Res. Technol.* **13**(1), 19–24 (2007).

8. F. H. Sakamoto et al., "Porphyrin distribution after topical aminolevulinic acid in a novel porcine model of sebaceous skin," *Lasers Surg. Med.* **41**(2), 154–160 (2009).
9. G. W. Lu et al., "Comparison of artificial sebum with human and hamster sebum samples," *Int. J. Pharm.* **367**(1–2), 37–43 (2009).
10. A. Teichmann et al., "Differential stripping: determination of the amount of topically applied substances penetrated into the hair follicles," *J. Invest. Dermatol.* **125**(2), 264–269 (2005).
11. R. L. Bronaugh, R. F. Stewart, and E. R. Congdon, "Methods for *in vitro* percutaneous absorption studies. II. Animal models for human skin," *Toxicol. Appl. Pharmacol.* **62**(3), 481–488 (1982).
12. A. C. Lauer et al., "Targeted delivery to the pilosebaceous unit via liposomes," *Adv. Drug Deliv. Rev.* **18**(3), 311–324 (1996).
13. P. J. Caspers et al., "*In vivo* confocal Raman microspectroscopy of the skin: noninvasive determination of molecular concentration profiles," *J. Invest. Dermatol.* **116**(3), 434–442 (2001).
14. A. Tfayli et al., "Follow-up of drug permeation through excised human skin with confocal Raman microspectroscopy," *Eur. Biophys. J.* **36**(8), 1049–1058 (2007).
15. G. Zhang, C. R. Flach, and R. Mendelsohn, "Tracking the dephosphorylation of resveratrol triphosphate in skin by confocal Raman microscopy," *J. Control Release* **123**(2), 141–147 (2007).
16. C. Adlhart and W. Baschong, "Surface distribution and depths profiling of particulate organic UV absorbers by Raman imaging and tape stripping," *Int. J. Cosmetic Sci.* **33**(6), 527–534 (2011).
17. G. Zhang, L. Senak, and D. J. Moore, "Measuring changes in chemistry, composition, and molecular structure within hair fibers by infrared and Raman spectroscopic imaging," *J. Biomed. Opt.* **16**(5), 056009 (2011).
18. A. Finlay and R. Marks, "Determination of corticoid concentration profiles in stratum corneum using the skin surface biopsy technique," *Br. J. Derm.* **107**(33), (1982).
19. B. W. Barry, H. G. M. Edwards, and A. C. Williams, "Fourier-transform Raman and Infrared vibrational study of human skin—assignment of spectral bands," *J. Raman Spectrosc.* **23**(11), 641–645 (1992).
20. L. Silveira et al., "Discriminating model for diagnosis of basal cell carcinoma and melanoma *in vitro* based on the Raman spectra of selected biochemicals," *J. Biomed. Opt.* **17**(7), 077003 (2012).
21. H. G. M. Edwards, D. E. Hunt, and M. G. Sibley, "FT-Raman spectroscopic study of keratotic materials: Horn, hoof and tortoiseshell," *Spectrochim. Acta. A* **54**(5), 745–757 (1998).
22. G. Socrates, *Infrared and Raman Characteristic Group Frequencies: Tables and Charts*, Wiley & Sons, West Sussex (2004).